

Supplementary information file associated to:

Traumatic brain injury promotes neurogenesis at the cost of astrogliogenesis in the adult hippocampus of male mice.

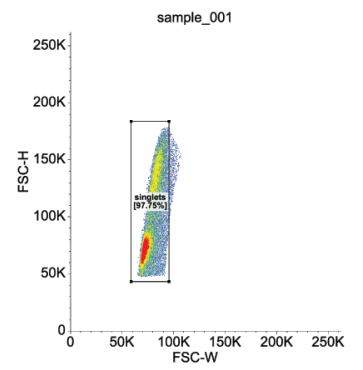
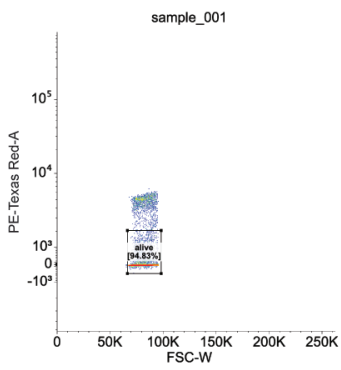
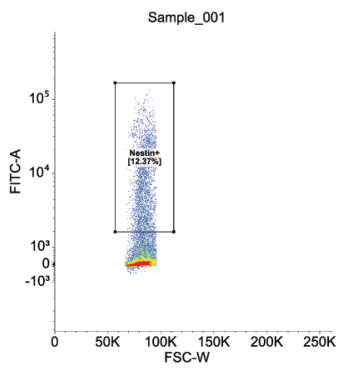
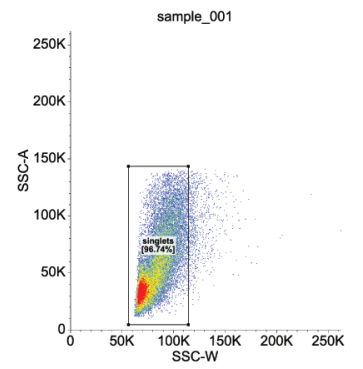
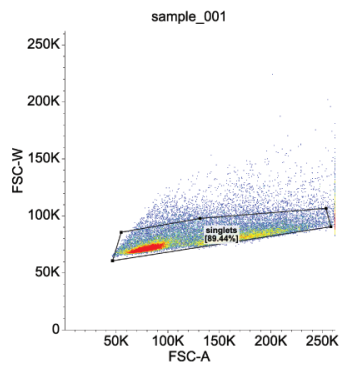
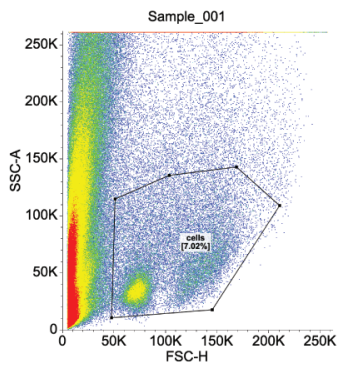
Nature Communications, 2024

Authors

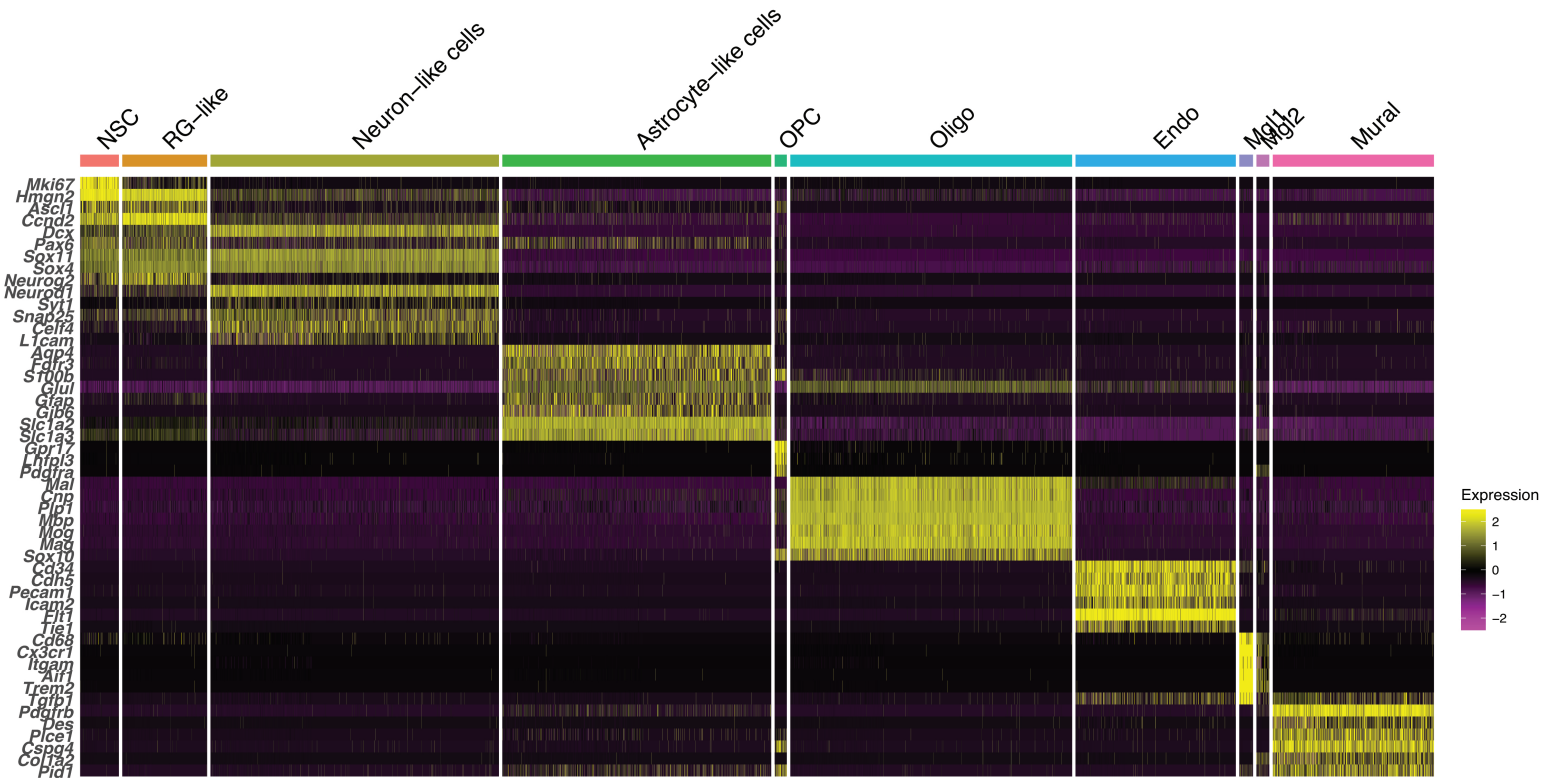
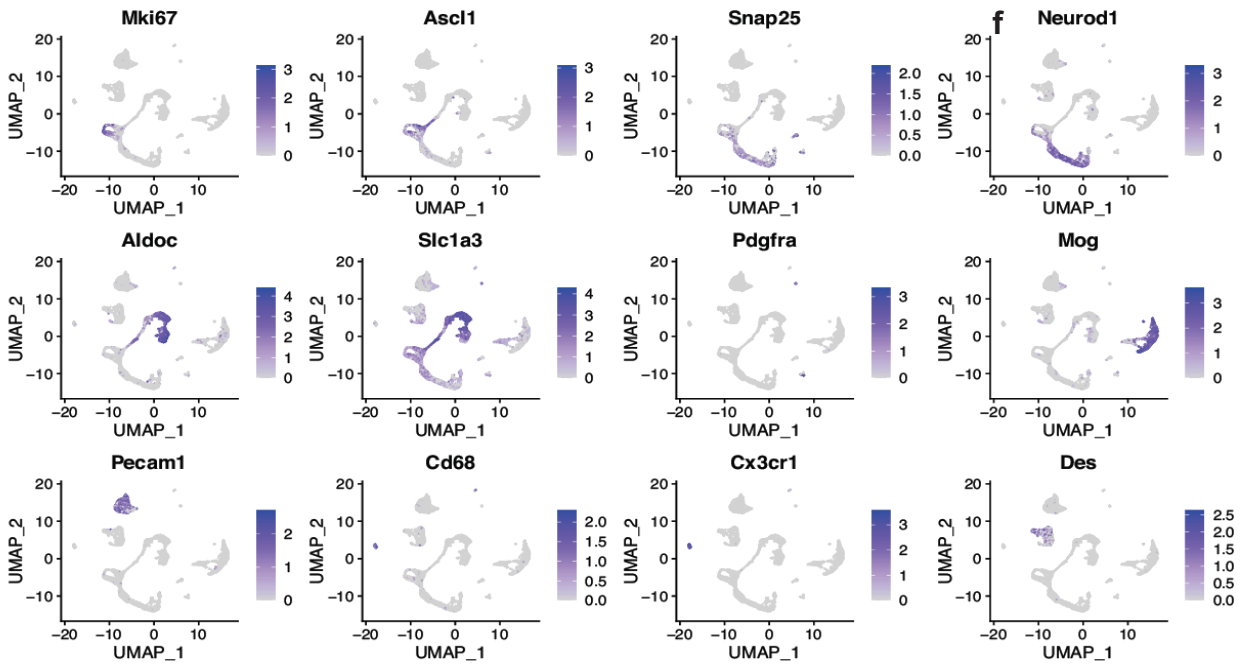
Bielefeld P, Martirosyan A, Martín-Suárez, S, Apresyan A, Meerhoff GF, Pestana F, Poovathingal S, Reijner N, Koning W, Clement RA, Van de Veen I, Toledo E, Polzer O, Durá I, Hovhannisyan S, Nilges B, Bogdoll A, Kashikar N, Lucassen PJ, Belgard TG, Encinas JM, Holt MG, Fitzsimons CP.

Contents

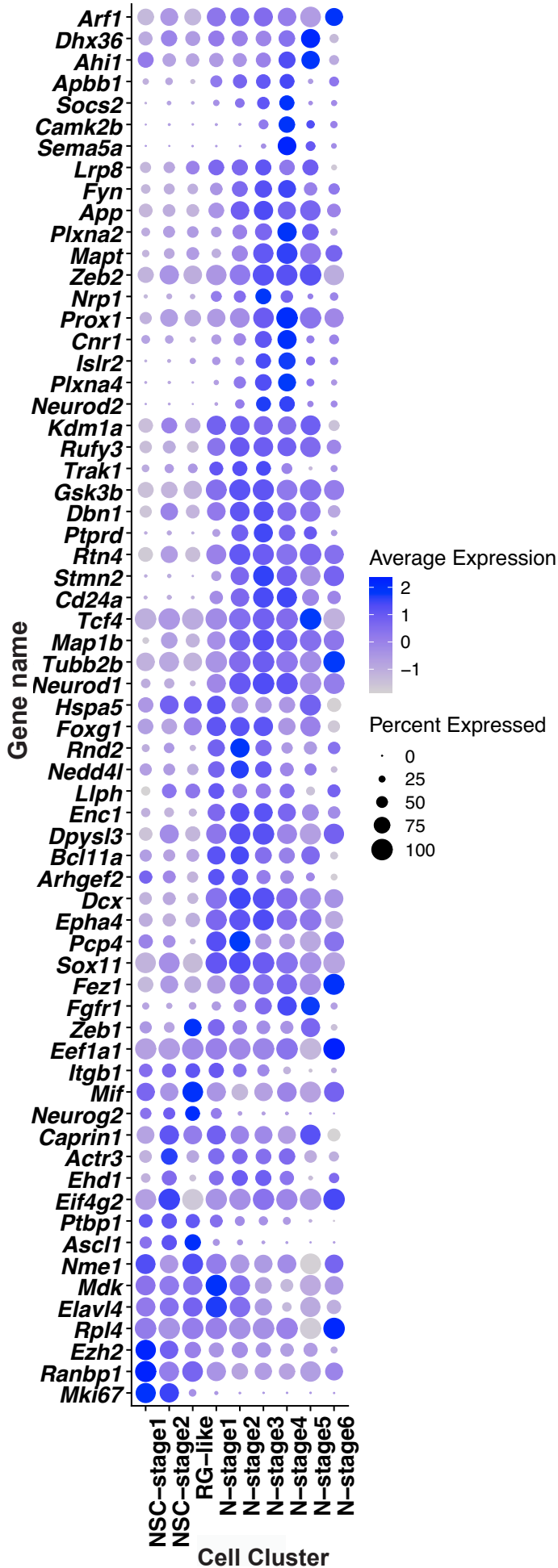
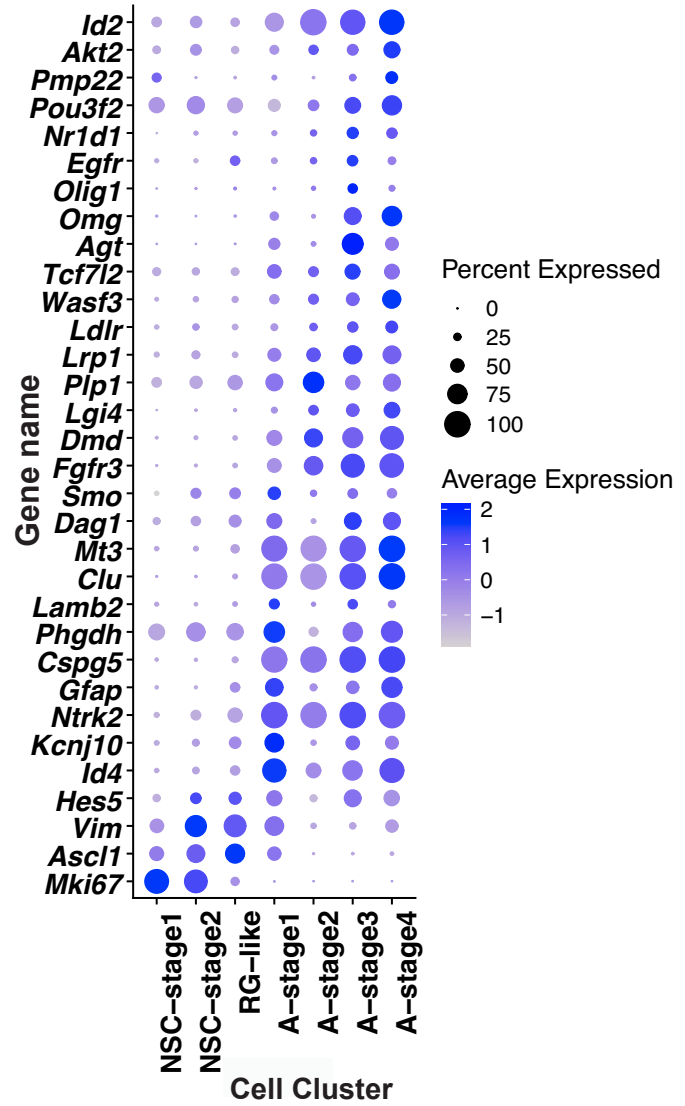
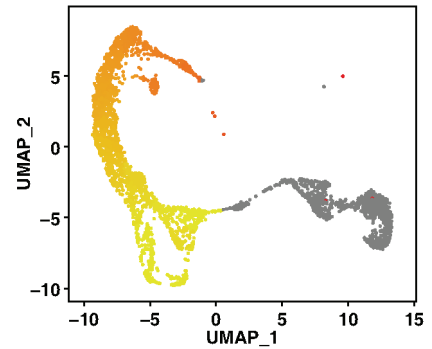
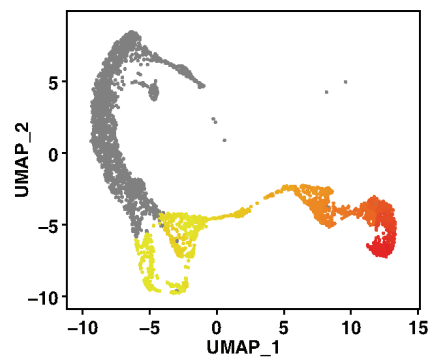
Supplementary figures 1-7 and legends to supplementary figures 1-7, summarizing their content.



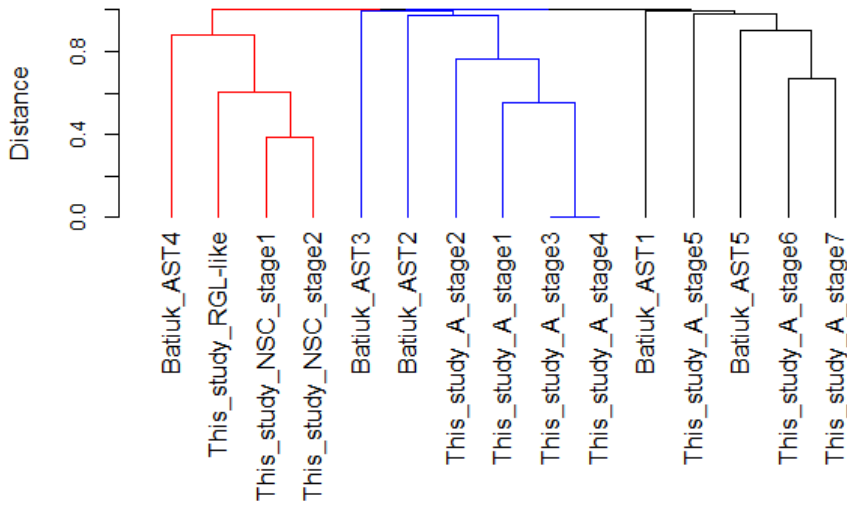
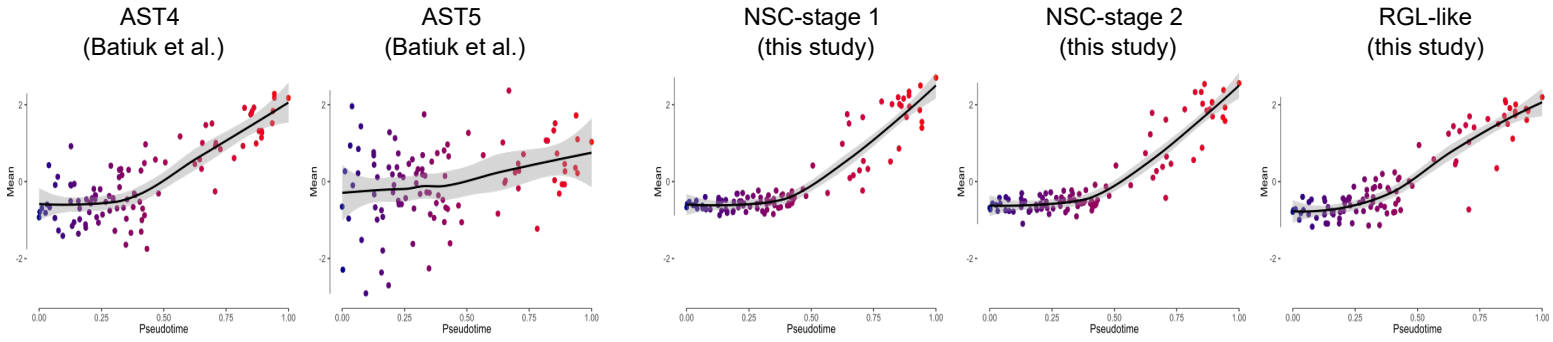
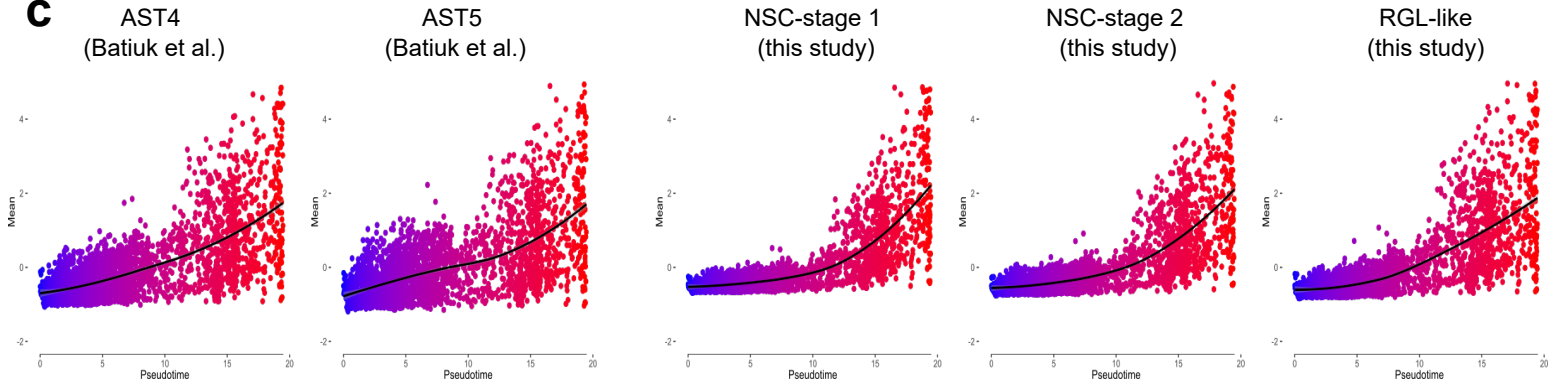
Legend to Supplementary Figure 1. Gating strategy used for FACS-based purification of GFP+ cells. Cells were initially selected using Forward and Side Scatter area plots (FSC-A and SSC-A) (indicated gate). To minimize the amount of small debris collected, care was taken to adjust the lower limit on the forward scatter (measure of size) axis, although the gate was left wide enough that smaller cells were still captured. Cell doublets were excluded using forward/side scatter width vs height plots (FSC-W/FSC-H and SSC-W/SSC-H). Live-dead staining using propidium iodide was used to identify viable cells, which were subsequently separated into GFP+ and GFP- populations based on fluorescence. GFP+ cells were retained for further use.

a**b**

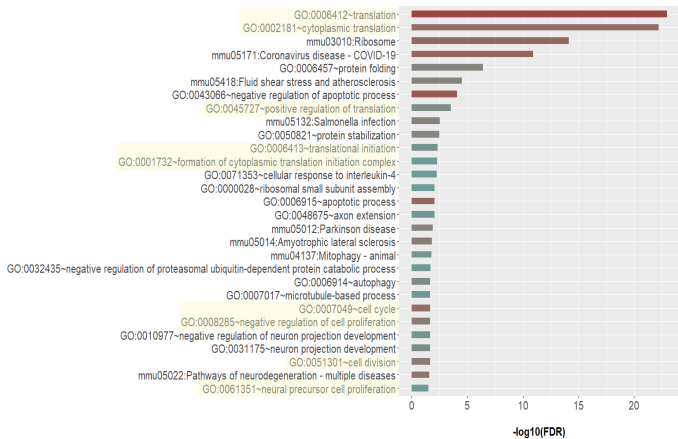
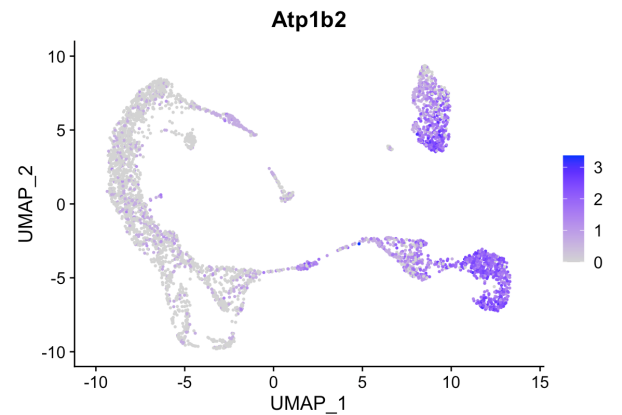
Legend to Supplementary Figure 2. Cell type assignment based on specific marker gene expression. Gene expression heatmap for higher-order cell types (columns) grouped according to the Seurat classification shown in Fig. 2a. Color-coding from Fig. 2a is retained. Magenta, low expression; yellow, high expression, ln-normalized gene expression data is shown. UMAP representations showing expression patterns of indicated marker genes across cell clusters (b), color bars indicate relative intensity of expression, SCT normalized values are shown.

a**b****c****d**

Legend to Supplementary Figure 3. Pseudotime assignment of NSC-derived cell lineages defined by expression of specific marker genes. Dot-plot graphs indicating the relative expression of marker genes in NSCs and NSC-derived neuronal (a) and astrocytic (b) populations; scaled SCT normalized data are shown. Color bars represent relative intensity of gene expression, dot size represents percentage of cells within an individual cell cluster (identity) expressing the indicated marker gene (feature). UMAP representations showing NSC-derived neuronal (c) and astrocytic lineages (d); color bars indicate calculated pseudotime distances from NSCs (yellow: minimum, red: maximum).

a**b****c****d**

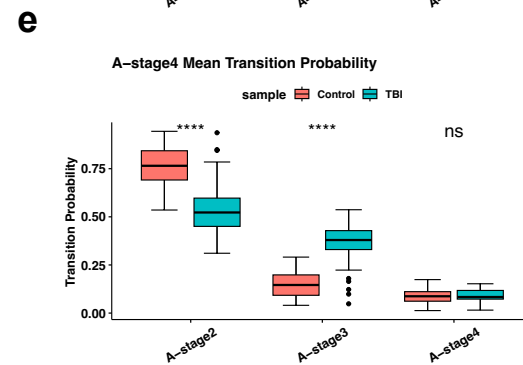
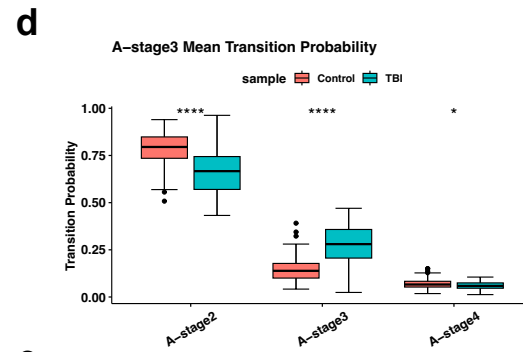
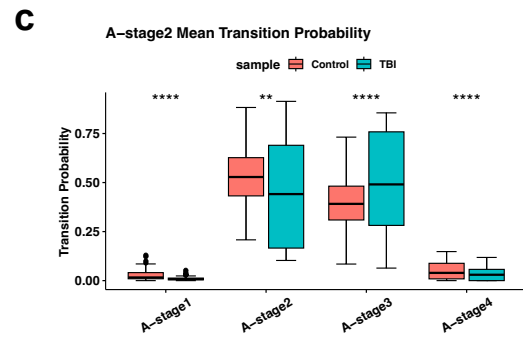
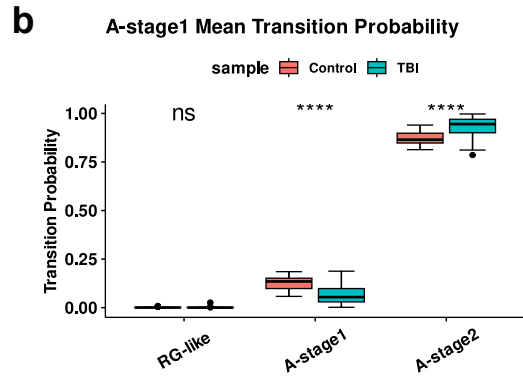
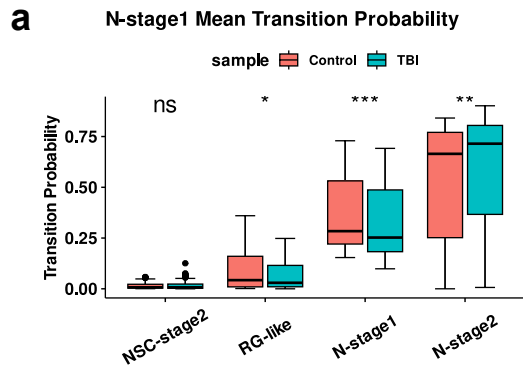
Batiuk AST4 cluster
 GO term + KEGG analysis with DAVID
 All terms FDR corrected $p_{val} < 0.05$

**e**

Legend to Supplementary Figure 4. Integrated analysis of hierarchical clustering, pseudotime profiles, and functional annotations for cell populations. Dendrogram showing hierarchical clustering of putative cell populations identified in Batiuk et al.³⁷, or in this study (a). The labels indicate the original group names. Genes in the indicated cell populations were plotted based on the pseudotime of Shin et al.²⁷ (b) and of Harris et al.²⁹ (c). The y-axis in (b) and (c) represents the mean z-score normalization of gene expression. The genes used to identify the AST4, AST5, NSC-stage 1, NSC-stage 2 and RG-like populations were extracted from the gene lists provided with each study and the mean value was calculated. GO biological pathway analysis using DAVID for the cell cluster AST4 identified in Batiuk et al.³⁷ FDR: false discovery rate (d). UMAP-based visualization of NSC-derived neuronal and astrocytic lineages with *Atp1b2* expression superimposed. Each dot represents an individual cell and gene expression is indicated by color intensity (e).

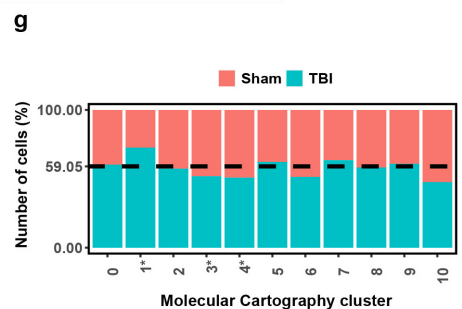
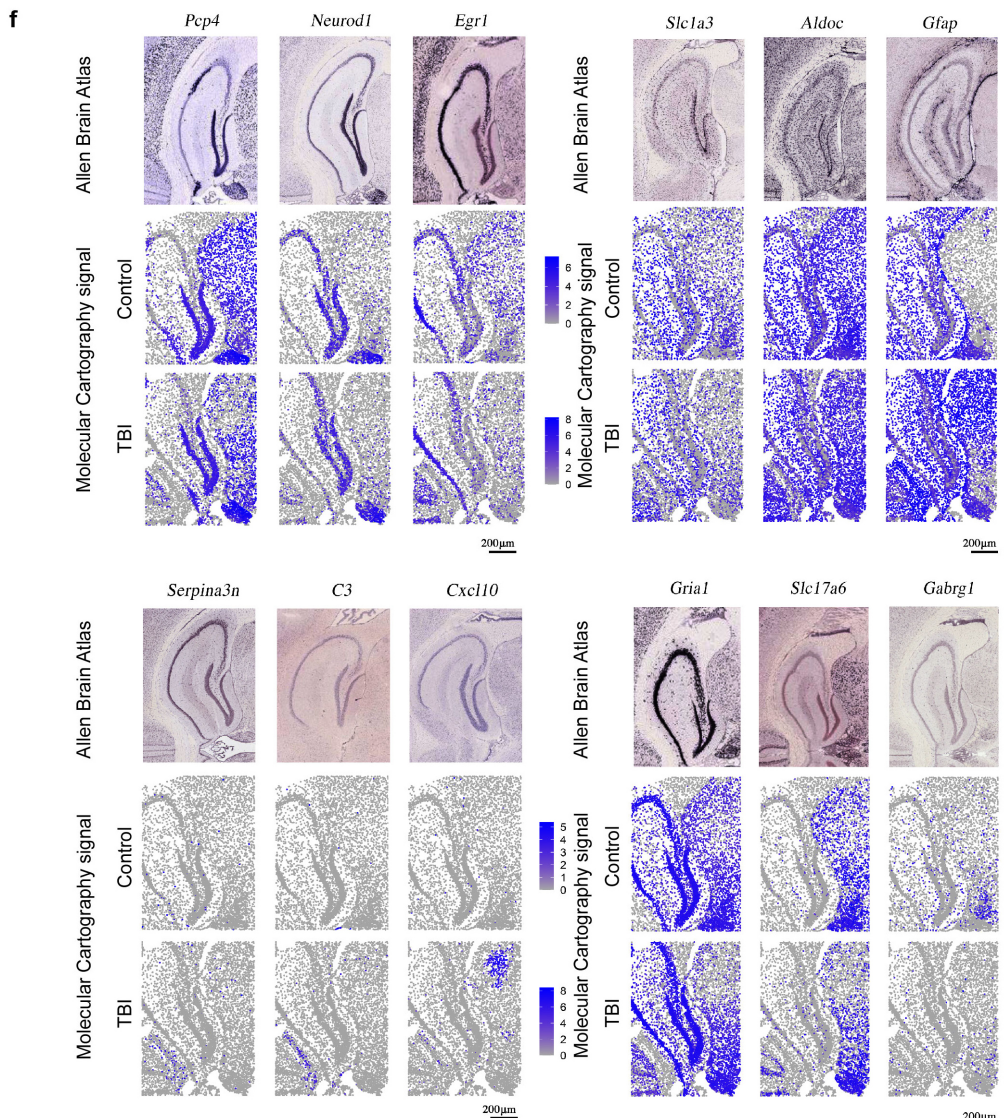
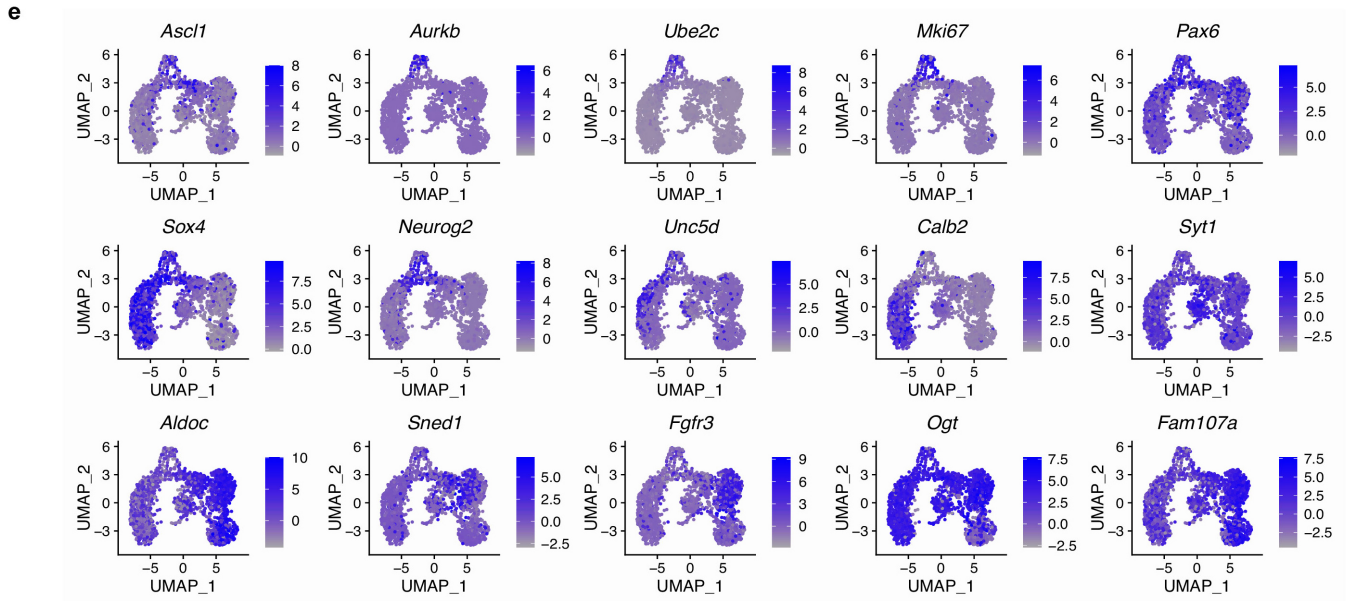
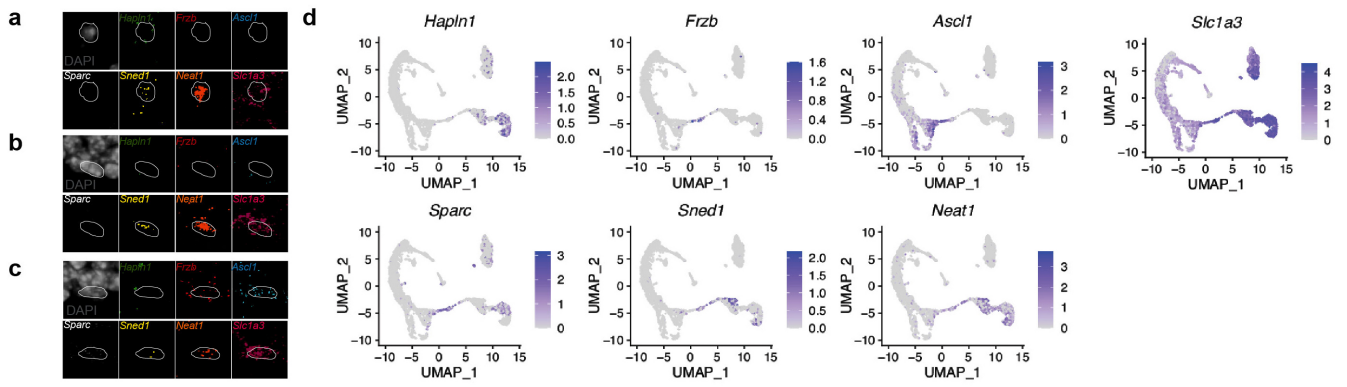
a**b**

Legend to Supplementary Figure 5. GO biological pathway matrix for the differentially expressed genes in NSC-derived cell populations. Differentially over-represented (red, $p < 0,05$) biological pathways found in the neuronal (a) and astrocytic (b) lineages.



Legend to Supplementary Figure 6. RNA velocity analysis of additional cell populations.

Box plots showing transition probabilities calculated for N-stage 1 cells (a), A-stage 1 cells (b), A-stage 2 cells (c), A-stage 3 cells (d) and A-stage 4 cells (e). Orange bars: Control group, cyan bars: TBI group, 5-6 animals per condition. In all panels, ns: $p > 0.05$; * $p < 0.05$; ** $p \leq 0.01$; *** $p \leq 0.001$; **** $p \leq 0.0001$, independent two-sided non-parametric Wilcoxon test. Exact p values for all statistical comparisons and calculated mean transition probabilities across cell clusters are available as Supplementary data 14. Box plots show the median, first quartile (25%), third quartile (75%) and inter-quartile range. Whiskers represent data minima and maxima; dots are data points located outside the whiskers. Source data is available as Supplementary data 15.



Legend to Supplementary Figure 7. Design and validation of probes for spatial transcriptomics. Sample confocal images representative of three independent experiments of RNA scope detection of marker genes used to identify individual A-stage 4 (a), A-stage 2 (b) and A-stage 1 (c) cells in the dentate gyrus. UMAP plots showing the expression of individual gene markers used for RNAscope validation, across astrocytic cell clusters, SCT normalized values are shown (d). UMAP representations of the combined 10X and Molecular Cartography dataset, indicating expression of exemplar marker genes for the various identified cell populations (e). Sample images representative of three independent experiments showing how mRNA expression detected by 12 probes in Molecular Cartography experiments compares to that reported in the Allen Brain Atlas, colored bars indicate relative intensity of gene expression, raw counts are shown, colored dots indicate individual cells in the dentate gyrus(f). Bar plots showing the relative number of cells per identified Molecular Cartography cluster in Control or TBI samples, against their expected abundance (based on 59,05% of all cells originating from TBI samples: dashed line), * $p < 0.05$ vs. expected abundance, binomial test (g). The numbers of cells per cluster and experimental condition, and the statistical analyses performed are given in Supplementary data 11, including exact p values for all statistical comparisons.